# Chapter 7

# Production of CO and $CO_2$ in the Photolysis of Ice Core Contaminants by Cerenkov Radiation of Cosmic Origin

## Introduction

In order to test our hypothesis, that *in situ* production of CO and $CO_2$ from the photolysis of chromophoric organic matter is feasible, we now present a series of calculations as integrated functions of time, depth, photon flux from Cerenkov radiation, and measured quantum yields. We will initially estimate the photon flux produced by Cerenkov radiation penetrating through ice and then establish a correlation between organic matter typically found in ice with the measured quantum efficiencies of Chapter 6. This will allow us to estimate the potential production of CO and $CO_2$ in ice cores as a function of depth (e.g., time).

## Cerenkov Radiation in Ice: Origin and Quantification in the Action Spectral Range

The penetration of high-energy cosmic particles in the Earth's atmosphere produces energetic neutrinos and muons. Approximately, $F = 0.01$ energetic muons $cm^{-2}$ $s^{-1}$ with kinetic energies $T > 0.1$ GeV continuously hit the Earth's surface; a significant fraction of these cosmic rates penetrate deep into the Earth's crust with a substantial fraction emerging on the opposite earth side of entry.[1] Given that muons move at a velocity, $\nu$, that is larger than the speed of light in ice, $\nu_i$, they induce a macroscopic polarization field in a plane perpendicular to their trajectory. The generated polarization field is formed in response to the temporary loss of electroneutrality within a volume element. As a consequence of an associated relaxation due to the transient polarization, there is an

emission of Cerenkov radiation (i.e., UV radiation) over the wavelength range of $\lambda$ = 200 to 400 nm as the energetic muons penetrate into ice as a function of depth.

The fraction of muons which are Cerenkov-active ($\beta = \nu/c$), or move faster than the speed of light in ice, can be determined from eq. 7-1 as follows:

$$\beta = \sqrt{1 - \frac{1}{[1 + (T / m_0 c^2]^2}} \tag{7-1}$$

where $m_0 = 1.88 \times 10^{-28}$ Kg is the mass of a muon, i.e., about 206 times heavier than the electro, and $c = 3 \times 10^8$ km $s^{-1}$ is the speed of light. Given that ice has a refractive index of $n \sim 1.32$ over the UV spectral region, the speed of light in ice is therefore $\nu_i = c/n = 0.756\ c$. As a consequence, muons with velocity of $\nu > 1.32\ \nu_i$ will emit Cerenkov radiation as they penetrate through ice. Furthermore with $m_0 c^2$ = 105 MeV, we can estimate via eq. 7-1 that 86% of muons with $T > 0.1$ GeV are Cerenkov emitters.

The fundamental equation of the Cerenkov emission is written as follows:[2]

$$\frac{dN}{d\lambda} = -2\pi\gamma\left(1 - \frac{1}{\beta^2 n^2}\right)\frac{1}{\lambda^2} \tag{7-2}$$

where $\gamma$ = 1/137 is a dimensionless fine structure constant, $n$ is the average refractive index of the medium (i.e., ice), and $dN$ is the number of photons emitted by each muon over the wavelength interval [$\lambda + d\lambda$] per cm of penetration. The flux of photons, which are generated in ice cores, is estimated for muons with $T > 1$ GeV and $\beta > 0.996 > 0.756$. Under these conditions given the surficial muon flux of $F = 0.01$ muons $cm^{-2}$ $s^{-1}$ with $\beta \sim$

1, $dR_{Cerenkov}$ = 1900 photons $\lambda^{-2}\, d\lambda$ $cm^{-3}$ $s^{-1}$ $nm^{-1}$. However, muons are poorly attenuated in transparent, crystalline glacial ice. For example, they have been shown to travel for several hundred of meters before their kinetics energies drop below the Cerenkov emission threshold. This mechanism represents a permanent and homogeneous source of short-wavelength photons at all depths. In contrast, sunlight is completely attenuated in the first 20 cm of surface snow.

**Absorption and Scattering of Photons in Ice**

Cerenkov radiation emitted by energetic neutrinos has been measured as a part of the AMANDA (Antarctic Neutrino and Muon Detector Array) project, which involves the detection of photons at depths of ~ 2 km.[3] In addition, the average distance that a photon emitted by Cerenkov radiation ($\lambda$ = 350 nm) in glacial ice is approximately 120 m from the time it was generated until detection.[4] Likewise, from measurements of the photon arrival-time distributions at an array of detectors positioned at variable distances from a pulsed, diffuse, monochromatic source, the intrinsic absorption and scattering coefficients of ice have been determined.[5] From these measurements, light scattering was determined to be the result of interactions of photons with residual air bubbles. When a photon traveling in a random walk in ice reaches an ice/bubble interface, it is is scattered into a new random walk. Absorption of photons was determined to be controlled by chemical impurities and by self-absorption of ice.

Photon absorption by ice in the near-UV is due to excitation of $H_2O$ intra- and inter-molecular vibrational overtones.[5] Bellow 500 nm absorption coefficients in ice are negligible because the probability of multi-photon processes decrease exponentially.

The wavelength-dependent absorption coefficient of glacial ice can be estimated from the following empirical relationship:

$$\alpha(\lambda) = A\exp(-0.482\,\lambda) + B\exp(-6700/\lambda) + C\,\lambda^{-1.1} \qquad (7\text{-}3)$$

where $A = 8 \times 10^{37}$ cm$^{-1}$, $B = 81$ cm$^{-1}$, and $C = 0.0347$ cm$^{-1}$ for relatively clean Antarctic ice at depths below ~ 1500 m.[6] The empirical coefficient C depends on the concentration of impurities in ice that impact light absorption and the effective scattering coefficient.

**Organic Matter in Ice**

The polar ice caps are known to be contaminated by organic material of continental or marine origin including the deposition of the organic aerosol released by major, sporadic, boreal forest fires.[7-12] Full speciation of the organic matter present in polar ice remains a daunting analytical challenge,[13] but it is agreed that the organic contaminants largely consist of humic-like substances, such as those that are globally present in natural waters, the simpler products of their solar photodegradation,[14-18] as well as the products of organic aerosol photooxidation, such as dicarboxylic, α- and ω-oxocarboxylic acids, and α-dicarbonyl species.[19-22]

Dissolved organic matter (DOM) isolated from cloud water is acidic and polyfunctional, and absorbs UV radiation in the 200–450 nm range. This pool of DOM consists of dialkyl ketones and diketones, alkanedioic acids, hydroxyalkanoic acids, and macromolecular polycarboxylic acids such as fulvic acids, which are analogous to the species detected in Antarctic and Arctic snow and ice samples. For example, a series of homologous α- and ω-oxocarboxylic acids, ketocarboxylic acids, and dicarbonyls have been identified and characterized in Greenland ice core samples (206 m depth, 450 years old),[11] including pyruvic acid. However, these species account only for ~ 5% of the total organic carbon content (TOC) of ice, [TOC] = (1.8 ± 1.0) μg TOC $g^{-1}$ ice, or assuming an ice density of δ = 0.916 g $cm^{-3}$ [TOC] = (1.7 ± 0.9) μg TOC $cm^{-3}$ ice. This concentration is sufficient to generate considerable excesses of CO and $CO_2$, i.e., 20 ppmv $CO_2 \simeq 0.87$ ηg C $g^{-1}$ ice. The remainder is believed to consist of the DOM found in natural aquatic environments, and in soil.[13]

We expect that a significant fraction of DOM in polar ice (i.e., Eurocore, GRIP, T = –32 ºC) samples to be dissolved in highly viscous aqueous microfluid environments, the so-called quasi-liquid layer, where the solutes are photoreactive (e.g., pyruvic acid).[23]

A high-resolution study of the organic matter versus depth (i.e., time back to 1193 AD) at the Summit site in central Greenland indicates several sharp spikes in the concentration of oxalate and formate, which may have been derived from higher molecular weight DOM.[12] In the southern hemisphere, TOC levels have kept relatively

constant for the last thousand years. Substantially less organic material was found in Antarctic ice from the Holocene.[24]

**Absorption Coefficients and Quantum Yields of CO and $CO_2$ from the Photolysis of Dissolved Organic Matter (DOM) in Surface Ocean**

A Gaussian function can be fitted to represent the absorption coefficient ε (base 10) of DOM above $\lambda \geq 200$ nm from data reported by Zuo and Jones as shown in equation 7-4.[25]

$$\varepsilon = 1.39 \times 10^4 \exp\left\{-0.5\left[\left(\lambda - 153.5\right)/115.3\right]^2\right\} \qquad (7\text{-}4)$$

From eq. 7-4 it is clear that the absorption coefficient increases sharply at shorter wavelengths.

The photochemical degradation of DOM in the atmosphere, surface waters, and snow/ice[26,27] yields CO,[18,28,29] and $CO_2$.[30] Quantum yields for CO photoproduction from DOM, $\phi_{CO}$, decay exponentially with λ, $\phi_{CO} = \exp(-2.68 - 0.020\,\lambda)$.[16] In addition, the quantum yield of $CO_2$ production from DOM photolysis in natural waters has been reported for open, costal, and inshore ocean to be: $\phi_{CO_2} = \exp\{-[5.53 + 0.00914\ (\lambda - 290)]\}$, $\phi_{CO_2} = \exp\{-[6.36 + 0.0140\ (\lambda - 290)]\}$, and $\phi_{CO_2} = \exp\{-[6.66 + 0.0285\ (\lambda - 290)]\}$, respectively.[30] In a similar fashion, natural organic matter in ice is expected to be

photodegraded into CO, $CO_2$, and simple ketocarboxylic species, which may, in turn, undergo further photolysis.

**Rates of DOM Photolytic Decarboxylation and Decarbonylation: Comparison of Experimental Values in Ice vs. Ice Core Model Results**

For a model of organic matter photolysis in ice cores, we first consider a thin layer of chromophoric impurities that are embedded in bubbly, dusty ice cores as described by Askebjer et al. (1997),[31] from which we can estimate the rate of absorption of Cerenkov ultraviolet radiation. The net trajectories of photons penetrating through ice are characterized by random walks with scattering and absorption lengths, $\Gamma_s$ and $\Gamma_a$, respectively. At depth of 500 m, $\Gamma_s \sim 10$ cm which leads to a diffusion coefficient: $D = \nu_i \Gamma_s / 3 = 8 \times 10^{10} \text{cm}^2 \text{s}^{-1}$. For a diffusive process involving attenuation, with an average path $l$ traveled by a photon between two points separated by a distance $z$, we can write the following equation:

$$l = \frac{\sqrt{3}}{2} \sqrt{\frac{\Gamma_a}{\Gamma_s} z} \tag{7-5}$$

In this case, $l$ and $z$ are both proportional to the time $t$ (i.e., $t$ and $t^{1/2}$, respectively) for diffusion in a transparent medium ($\Gamma_a \rightarrow \infty$). As a consequence, photons will be attenuated as a function of $\exp(-l/\Gamma_a)$, over a scale $\Gamma_{eff} = 2\ (\Gamma_a\ \Gamma_s/3)^{1/2}$. For pure or undoped ice: $\Gamma_{a,ice} = 1/\alpha(\lambda) \sim 18 \times 10^3$ cm, $\Gamma_{eff,ice} = 490$ cm at $\lambda = 350$ nm. Furthermore, the average lifetime for photons produced faraway from the absorbing layer is $\tau =$

$\Gamma_{a,ice}/\nu_i$, which leads to a spectral photon density $dU_{ice} = (\Gamma_{a,ice}/\nu_i)\ dR_{Cerenkov} = 1900\ (\Gamma_{a,ice}/\nu_i)\ \lambda^{-2}\ d\lambda$ photons cm$^{-3}$ nm$^{-1}$.

Enhanced photon absorption by the embedded chromophoric impurities creates a depletion layer, $\Gamma_{a,layer} = 1/(\varepsilon(\lambda)\ [DOC])$ that for the Greenland ice sections, has an average value of $\Gamma_{a,layer} \sim 180$ cm at 350 nm, leading to an $\Gamma_{eff,layer} = 50$ cm, $\tau = 50$ ns. In general, $dU_{layer} = (\Gamma_{a,layer}/\nu_i)\ dR_{Cerenkov} = 1900\ (\Gamma_{a,layer}/\nu_i)\ \lambda^{-2}\ d\lambda$ photons cm$^{-3}$ nm$^{-1}$ $\ll dU_{ice}$. The spectral photon flux $J_\lambda$ diffusing from bulk ice into the impurity stratum through twin depletion layers of thickness $\Gamma_{eff,layer}$ can be evaluated from (Figure 7-1):

$$J_\lambda d\lambda = 2D\frac{dU_{ice} - dU_{layer}}{\Gamma_{eff,layer}} \tag{7-6}$$

The overall rate of CO production (molecules cm$^{-3}$ ice year$^{-1}$) is given by the product $J_\lambda\ \phi(\lambda)\ d\lambda$ integrated over $[\lambda_1, \lambda_2]$:

$$\frac{d[CO]}{dt} = 4.2\times10^{11}\int_{\lambda_1}^{\lambda_2}\frac{\phi_{CO}(\lambda)}{\lambda^2}\left(\frac{\Gamma_{a,ice} - \Gamma_{a,layer}}{\Gamma_{eff,layer}}\right)d\lambda \tag{7-7}$$

where $\Gamma_{a,ice} = 1/\alpha(\lambda)$, $\Gamma_{a,layer} = 1/(\varepsilon(\lambda)\ [DOC])$, and $\Gamma_{eff,layer} = 2\ (\Gamma_{a,ice}\ \Gamma_s/3)^{1/2}$ and from the diffusion coefficient $D$, we can estimate $\Gamma_s \sim 10$ cm. If we convert the above equation to mixing ratios by assuming that the air content of ice is 90 cm$^3$ kg$^{-1}$ ice and the ice density $\delta_{ice} = 0.916$ g cm$^{-3}$, which corresponds to a number density of air in the ice core bubbles of $n_a = 2.03 \times 10^{18}$ molecules air cm$^{-3}$ ice, we obtain an expression for the overall rate of CO production (ppbv year$^{-1}$) as follows:

$$\frac{d[\mathrm{CO}]_{\mathrm{ppbv}}}{dt} = 210 \int_{\lambda_1}^{\lambda_2} \frac{\phi_{\mathrm{CO}}(\lambda)}{\lambda^2} \left( \frac{\Gamma_{\mathrm{a,ice}} - \Gamma_{\mathrm{a,layer}}}{\Gamma_{\mathrm{eff,layer}}} \right) d\lambda \qquad (7\text{-}8)$$

In the same way, we can write a similar rate equation for photolytic production of $CO_2$ (ppmv year$^{-1}$):

$$\frac{d[\mathrm{CO}_2]_{\mathrm{ppmv}}}{dt} = 0.210 \int_{\lambda_1}^{\lambda_2} \frac{\phi_{\mathrm{CO}_2}(\lambda)}{\lambda^2} \left( \frac{\Gamma_{\mathrm{a,ice}} - \Gamma_{\mathrm{a,layer}}}{\Gamma_{\mathrm{eff,layer}}} \right) d\lambda \qquad (7\text{-}9)$$

Our experimental quantum efficiency for the photodecarboxylation of pyruvic acid in ice is $\phi = 0.25$ at the average temperature of Eurocore, GRIP (Greenland) ice of $T_{\mathrm{Eurocore}}$ = 241 K.[32] In addition, we have measured the temperature dependence of this reaction and showed that the quantum yields in ice are approximately 58% of those in solution at room temperature. Therefore, we apply a correction factor to the quantum yield used in equation 7-9 of $\phi^{\mathrm{ice}} = 0.58 \times \phi^{\mathrm{fluid}}$. Although we do not know the dependence for CO production in ice vs. the aqueous phase, we apply the same correction factor in equation 7-8.

The integrand in equations 7-8 and 7-9 peaks around 210 nm and falls quasi-exponentially with λ before vanishing above 400 nm. Despite the small local photon production rates, the exceptional transparency of pristine glacial ice between 200 and 500 nm[5,31] allows chromophoric point impurities, such as those created by sporadic contamination from DOM, to be photochemically processed not only by locally generated photons, but also from those created elsewhere and collected onto the absorbing layer

after diffusing through the ice matrix. A strongly absorbing sink effectively acts as an antenna whose collection efficiency is proportional to the ratio of the thickness of the pristine layer to the effective thickness of the layer containing the organic chromophore, ($\Gamma_{a,ice}/\Gamma_{eff,layer}$). This ratio depends, in general, on dust levels in the ice, as well as on chromophore concentration and absorptivity.[33]

The experimental differences $\Delta CO_2$ (ppmv) between readings from Greenland (Eurocore, GRIP) and Antarctic (South Pole: D47, D57) ice core records versus date,[32] and the differences $\Delta CO$ between (ppbv) readings from Greenland (Eurocore, GRIP) and the average constant value (89 ppbv) for the period 1640–1870 AD in this ice core record versus date,[34] were plotted in Figure 6-7 (see Chapter 6) for the last thousand years. We showed that there is a significant positive correlation between these $\Delta CO_2$ and $\Delta CO$ excesses over the last thousand years, despite the apparent dispersion – due to intrinsic heterogeneity of the deposits, the analytical difficulties, associated with ice sampling and transport –, and the variability of TOC levels.

A linear regression of the experimental data $\Delta CO$ vs. time leads to a slope $S^{measured}(CO) = -9.14 \times 10^{-2}$ ppbv year$^{-1}$. For the $\Delta CO_2$ vs. time data, the slope is $S^{measured}(CO_2) = -1.98 \times 10^{-2}$ ppmv year$^{-1}$.

The results of our calculations, based on equations 7-8 and 7-9 for the combination $\{200 \leq \lambda \leq 400$ nm; [DOC] = $1.7 \times 10^{-6}$ g C cm$^{-3}$ ice; C = 0.0347 cm$^{-1}$; $\phi^{ice} = 0.58 \times \phi^{fluid}\}$ yield slopes of $S^{calculated}(CO) = -5.41 \times 10^{-2}$ ppbv year$^{-1}$ and a mean for the three $CO_2$ cases of $S^{calculated}(CO_2) = -1.37 \times 10^{-2}$ ppmv year$^{-1}$. With the assumption that the quantum yields for CO and $CO_2$ show a wavelength dependence at $\lambda > 200$ nm as extrapolated from fluid solutions at $\lambda > 300$ nm, and applying a correction factor of $\phi^{ice} =$

$0.58 \times \phi^{fluid}$, we can account for up to 59% ΔCO and 69% $\Delta CO_2$ – from an average of the three cases reported, inshore-, coastal-, and open-ocean-waters[30] – in Greenland samples. These excesses are positively linked and can be explained by *in situ* photolysis of chromophoric organic contaminants by Cerenkov radiation of cosmic origin.

The details are shown below in Tables 7-1 to 7-3. In Table 7-1, the results of our calculations of the quantum yields for $\phi_{CO}$ and $\phi_{CO_2}$ – inshore, coastal and open ocean – production as a function of wavelength are presented. Table 7-2 shows the values of $\alpha(\lambda)$, $\Gamma_{a,ice}$, $\varepsilon(\lambda)$, $\Gamma_{a,layer}$, and $\Gamma_{eff,layer}$ as a function of wavelength and Table 7-3 shows the results of the rates of CO and $CO_2$ production vs. wavelength, $d[CO]/dt$ and $d[CO_2]/dt$, obtained from equations 7-8 and 7-9. Using the results of our calculations presented in Table 7-3, we obtained the slopes (in ppbv $year^{-1}$ or ppmv $year^{-1}$, respectively) as the sum of each column multiplied by the correction factor 0.58.

**Conclusions**

In conclusion, we have quantitatively estimated the impact of quasi-solid phase photochemistry on historical ice-core records. $CO_2$ mixing ratios in older Greenland air bubbles increasingly exceed their contemporaneous Antarctic levels. CO data display a similar pattern.[34] Both phenomena imply *in situ* chemical processing, and signal the onset of significant contamination in Greenland ice sections deeper than 155 m by species that slowly release CO and $CO_2$ by several different reaction mechanisms including photolysis.[34]

The observed correlation between $CO_2$ and CO anomalies (i.e., $\Delta CO$ and $\Delta CO_2$) suggests that the in situ oxidation/decomposition of organic compounds contributes to these anomalies.[34] Photochemistry mediated by *in situ* photon production from Cerenkov radiation of cosmic origin[33] and subsequent photolysis of dissolved organic matter is proposed as a likely source of excess CO and $CO_2$ (i.e., photolytic decarbonylation and decarboxylation) in Greenland ice core air bubbles.

An alternative reaction pathway that may lead to CO and $CO_2$ production involves the heterogeneous catalytic decomposition of $H_2O_2$ on granular size goethite ($\alpha$-FeOOH), or other metal oxyhydroxides derived from aerosol deposition,[9] leading to the formation of hydroxyl radical via a surface-bound Fenton reaction, which in turn lead to the oxidation of DOM.

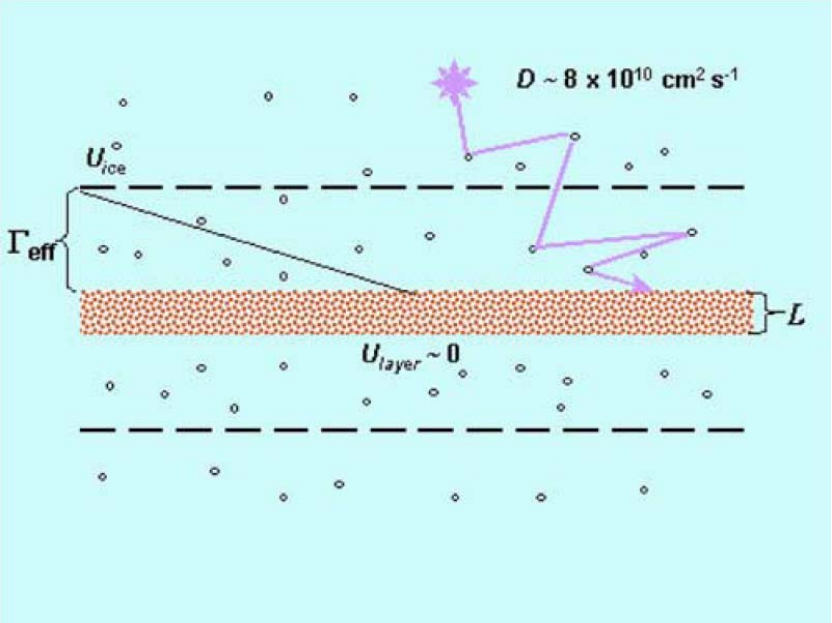


***Figure 7-1.*** Photons created over the ice core are scattered by gas bubbles, diffusing (photon densities: $U_{ice} \gg U_{layer}$) across depletion zones (thickness $\Gamma_{eff}$) towards the contaminated layer (thickness $L$), where they become absorbed by strongly chromophoric impurities. Reproduced from Ref. 33.

**Table 7-1.** Quantum yields of CO and $CO_2$ production from DOM photolysis in natural waters as a function of wavelength, $\phi_{CO} = \exp(-2.68 - 0.020\,\lambda)$,[16] and $\phi_{CO_2} = \exp\{-[5.53 + 0.00914\ (\lambda - 290)]\}$, $\phi_{CO_2} = \exp\{-[6.36 + 0.0140\ (\lambda - 290)]\}$, and $\phi_{CO_2} = \exp\{-[6.66 + 0.0285\ (\lambda - 290)]\}$, for open, costal, and inshore ocean respectively.[30]

| λ/nm | $10^3 \times \phi_{CO}$ | $10^3 \times \phi_{CO_2}$ inshore | $10^3 \times \phi_{CO_2}$ open ocean | $10^3 \times \phi_{CO_2}$ costal |
|---|---|---|---|---|
| 200 | 1.256 | 1.281 | 3.966 | 1.729 |
| 202 | 1.207 | 1.210 | 3.894 | 1.682 |
| 204 | 1.159 | 1.143 | 3.824 | 1.635 |
| 206 | 1.114 | 1.080 | 3.754 | 1.590 |
| 208 | 1.070 | 1.020 | 3.686 | 1.546 |
| 210 | 1.028 | 0.963 | 3.620 | 1.503 |
| 212 | 0.988 | 0.910 | 3.554 | 1.462 |
| 214 | 0.949 | 0.860 | 3.490 | 1.422 |
| 216 | 0.912 | 0.812 | 3.426 | 1.382 |
| 218 | 0.876 | 0.767 | 3.364 | 1.344 |
| 220 | 0.842 | 0.725 | 3.303 | 1.307 |
| 222 | 0.809 | 0.684 | 3.244 | 1.271 |
| 224 | 0.777 | 0.646 | 3.185 | 1.236 |
| 226 | 0.747 | 0.611 | 3.127 | 1.202 |
| 228 | 0.717 | 0.577 | 3.070 | 1.169 |
| 230 | 0.689 | 0.545 | 3.015 | 1.136 |
| 232 | 0.662 | 0.515 | 2.960 | 1.105 |
| 234 | 0.636 | 0.486 | 2.907 | 1.074 |
| 236 | 0.611 | 0.459 | 2.854 | 1.045 |
| 238 | 0.587 | 0.434 | 2.802 | 1.016 |
| 240 | 0.564 | 0.410 | 2.752 | 0.988 |
| 242 | 0.542 | 0.387 | 2.702 | 0.961 |
| 244 | 0.521 | 0.366 | 2.653 | 0.934 |
| 246 | 0.500 | 0.345 | 2.605 | 0.908 |
| 248 | 0.481 | 0.326 | 2.558 | 0.883 |
| 250 | 0.462 | 0.308 | 2.511 | 0.859 |
| 252 | 0.444 | 0.291 | 2.466 | 0.835 |
| 254 | 0.426 | 0.275 | 2.421 | 0.812 |
| 256 | 0.410 | 0.260 | 2.377 | 0.790 |
| 258 | 0.394 | 0.245 | 2.334 | 0.768 |
| 260 | 0.378 | 0.232 | 2.292 | 0.747 |
| 262 | 0.363 | 0.219 | 2.250 | 0.726 |
| 264 | 0.349 | 0.207 | 2.210 | 0.706 |
| 266 | 0.335 | 0.195 | 2.170 | 0.686 |
| 268 | 0.322 | 0.184 | 2.130 | 0.667 |
| 270 | 0.310 | 0.174 | 2.092 | 0.649 |

| | | | | |
|---|---|---|---|---|
| 272 | 0.298 | 0.165 | 2.054 | 0.631 |
| 274 | 0.286 | 0.155 | 2.017 | 0.614 |
| 276 | 0.275 | 0.147 | 1.980 | 0.597 |
| 278 | 0.264 | 0.139 | 1.944 | 0.580 |
| 280 | 0.254 | 0.131 | 1.909 | 0.564 |
| 282 | 0.244 | 0.124 | 1.874 | 0.549 |
| 284 | 0.234 | 0.117 | 1.840 | 0.534 |
| 286 | 0.225 | 0.110 | 1.807 | 0.519 |
| 288 | 0.216 | 0.104 | 1.774 | 0.504 |
| 290 | 0.208 | 0.099 | 1.742 | 0.491 |
| 292 | 0.199 | 0.093 | 1.711 | 0.477 |
| 294 | 0.192 | 0.088 | 1.680 | 0.464 |
| 296 | 0.184 | 0.083 | 1.649 | 0.451 |
| 298 | 0.177 | 0.078 | 1.619 | 0.439 |
| 300 | 0.170 | 0.074 | 1.590 | 0.426 |
| 302 | 0.163 | 0.070 | 1.561 | 0.415 |
| 304 | 0.157 | 0.066 | 1.533 | 0.403 |
| 306 | 0.151 | 0.062 | 1.505 | 0.392 |
| 308 | 0.145 | 0.059 | 1.478 | 0.381 |
| 310 | 0.139 | 0.056 | 1.451 | 0.371 |
| 312 | 0.134 | 0.053 | 1.425 | 0.361 |
| 314 | 0.128 | 0.050 | 1.399 | 0.351 |
| 316 | 0.123 | 0.047 | 1.374 | 0.341 |
| 318 | 0.119 | 0.044 | 1.349 | 0.331 |
| 320 | 0.114 | 0.042 | 1.324 | 0.322 |
| 322 | 0.109 | 0.040 | 1.300 | 0.313 |
| 324 | 0.105 | 0.037 | 1.277 | 0.305 |
| 326 | 0.101 | 0.035 | 1.254 | 0.296 |
| 328 | 0.097 | 0.033 | 1.231 | 0.288 |
| 330 | 0.093 | 0.032 | 1.209 | 0.280 |
| 332 | 0.090 | 0.030 | 1.187 | 0.272 |
| 334 | 0.086 | 0.028 | 1.165 | 0.265 |
| 336 | 0.083 | 0.027 | 1.144 | 0.258 |
| 338 | 0.079 | 0.025 | 1.123 | 0.251 |
| 340 | 0.076 | 0.024 | 1.103 | 0.244 |
| 342 | 0.073 | 0.022 | 1.083 | 0.237 |
| 344 | 0.070 | 0.021 | 1.064 | 0.230 |
| 346 | 0.068 | 0.020 | 1.044 | 0.224 |
| 348 | 0.065 | 0.019 | 1.025 | 0.218 |
| 350 | 0.063 | 0.018 | 1.007 | 0.212 |
| 352 | 0.060 | 0.017 | 0.989 | 0.206 |
| 354 | 0.058 | 0.016 | 0.971 | 0.200 |
| 356 | 0.055 | 0.015 | 0.953 | 0.195 |
| 358 | 0.053 | 0.014 | 0.936 | 0.189 |
| 360 | 0.051 | 0.013 | 0.919 | 0.184 |
| 362 | 0.049 | 0.013 | 0.902 | 0.179 |
| 364 | 0.047 | 0.012 | 0.886 | 0.174 |
| 366 | 0.045 | 0.011 | 0.870 | 0.169 |
| 368 | 0.044 | 0.011 | 0.854 | 0.165 |

| | | | | |
|---|---|---|---|---|
| 370 | 0.042 | 0.010 | 0.839 | 0.160 |
| 372 | 0.040 | 0.010 | 0.823 | 0.156 |
| 374 | 0.039 | 0.009 | 0.808 | 0.151 |
| 376 | 0.037 | 0.008 | 0.794 | 0.147 |
| 378 | 0.036 | 0.008 | 0.779 | 0.143 |
| 380 | 0.034 | 0.008 | 0.765 | 0.139 |
| 382 | 0.033 | 0.007 | 0.751 | 0.135 |
| 384 | 0.032 | 0.007 | 0.738 | 0.132 |
| 386 | 0.030 | 0.006 | 0.724 | 0.128 |
| 388 | 0.029 | 0.006 | 0.711 | 0.124 |
| 390 | 0.028 | 0.006 | 0.698 | 0.121 |
| 392 | 0.027 | 0.005 | 0.686 | 0.118 |
| 394 | 0.026 | 0.005 | 0.673 | 0.114 |
| 396 | 0.025 | 0.005 | 0.661 | 0.111 |
| 398 | 0.024 | 0.005 | 0.649 | 0.108 |
| 400 | 0.023 | 0.004 | 0.637 | 0.105 |

**Table 7-2.** Absorption coefficient of glacial ice, absorption lengths of undoped ice, absorption coefficient of dissolved organic matter, absorption lengths of the depletion layer in its vicinity, and effective absorption lengths of the depletion layer as a function of wavelength.

| $\lambda$/nm | $10^4 \times \alpha(\lambda)/cm^{-1}$ | $10^{-3} \times \Gamma_{a,ice}/cm$ | $10^3 \times \varepsilon/(cm^2\ g^{-1}$ DOM) | $\Gamma_{a,layer}/cm$ | $\Gamma_{eff,layer}/cm$ |
|---|---|---|---|---|---|
| 200 | 2.111 | 4.738 | 12.814 | 45.9 | 24.7 |
| 202 | 1.426 | 7.014 | 12.723 | 46.2 | 24.8 |
| 204 | 1.158 | 8.637 | 12.629 | 46.6 | 24.9 |
| 206 | 1.049 | 9.532 | 12.531 | 46.9 | 25.0 |
| 208 | 1.001 | 9.987 | 12.431 | 47.3 | 25.1 |
| 210 | 0.977 | 10.237 | 12.327 | 47.7 | 25.2 |
| 212 | 0.961 | 10.402 | 12.221 | 48.1 | 25.3 |
| 214 | 0.949 | 10.533 | 12.112 | 48.6 | 25.4 |
| 216 | 0.939 | 10.650 | 12.001 | 49.0 | 25.6 |
| 218 | 0.929 | 10.762 | 11.887 | 49.5 | 25.7 |
| 220 | 0.920 | 10.872 | 11.770 | 50.0 | 25.8 |
| 222 | 0.911 | 10.981 | 11.651 | 50.5 | 25.9 |
| 224 | 0.902 | 11.090 | 11.530 | 51.0 | 26.1 |
| 226 | 0.893 | 11.199 | 11.407 | 51.6 | 26.2 |
| 228 | 0.884 | 11.308 | 11.281 | 52.1 | 26.4 |
| 230 | 0.876 | 11.417 | 11.154 | 52.7 | 26.5 |
| 232 | 0.868 | 11.527 | 11.025 | 53.4 | 26.7 |
| 234 | 0.859 | 11.636 | 10.893 | 54.0 | 26.8 |
| 236 | 0.851 | 11.746 | 10.761 | 54.7 | 27.0 |
| 238 | 0.844 | 11.855 | 10.626 | 55.4 | 27.2 |
| 240 | 0.836 | 11.965 | 10.491 | 56.1 | 27.3 |
| 242 | 0.828 | 12.074 | 10.353 | 56.8 | 27.5 |
| 244 | 0.821 | 12.184 | 10.215 | 57.6 | 27.7 |
| 246 | 0.813 | 12.294 | 10.075 | 58.4 | 27.9 |
| 248 | 0.806 | 12.404 | 9.935 | 59.2 | 28.1 |
| 250 | 0.799 | 12.514 | 9.793 | 60.1 | 28.3 |
| 252 | 0.792 | 12.624 | 9.650 | 61.0 | 28.5 |
| 254 | 0.785 | 12.735 | 9.507 | 61.9 | 28.7 |
| 256 | 0.779 | 12.845 | 9.363 | 62.8 | 28.9 |
| 258 | 0.772 | 12.955 | 9.218 | 63.8 | 29.2 |
| 260 | 0.765 | 13.066 | 9.073 | 64.8 | 29.4 |
| 262 | 0.759 | 13.176 | 8.927 | 65.9 | 29.6 |
| 264 | 0.753 | 13.287 | 8.782 | 67.0 | 29.9 |
| 266 | 0.746 | 13.398 | 8.635 | 68.1 | 30.1 |
| 268 | 0.740 | 13.509 | 8.489 | 69.3 | 30.4 |
| 270 | 0.734 | 13.620 | 8.343 | 70.5 | 30.7 |

| | | | | | |
|---|---|---|---|---|---|
| 272 | 0.728 | 13.731 | 8.197 | 71.8 | 30.9 |
| 274 | 0.722 | 13.842 | 8.051 | 73.1 | 31.2 |
| 276 | 0.717 | 13.953 | 7.905 | 74.4 | 31.5 |
| 278 | 0.711 | 14.064 | 7.759 | 75.8 | 31.8 |
| 280 | 0.705 | 14.175 | 7.614 | 77.3 | 32.1 |
| 282 | 0.700 | 14.286 | 7.470 | 78.7 | 32.4 |
| 284 | 0.695 | 14.398 | 7.326 | 80.3 | 32.7 |
| 286 | 0.689 | 14.509 | 7.182 | 81.9 | 33.0 |
| 288 | 0.684 | 14.620 | 7.039 | 83.6 | 33.4 |
| 290 | 0.679 | 14.732 | 6.897 | 85.3 | 33.7 |
| 292 | 0.674 | 14.843 | 6.756 | 87.1 | 34.1 |
| 294 | 0.669 | 14.955 | 6.616 | 88.9 | 34.4 |
| 296 | 0.664 | 15.067 | 6.476 | 90.8 | 34.8 |
| 298 | 0.659 | 15.178 | 6.338 | 92.8 | 35.2 |
| 300 | 0.654 | 15.290 | 6.201 | 94.9 | 35.6 |
| 302 | 0.649 | 15.401 | 6.065 | 97.0 | 36.0 |
| 304 | 0.645 | 15.513 | 5.930 | 99.2 | 36.4 |
| 306 | 0.640 | 15.624 | 5.796 | 101.5 | 36.8 |
| 308 | 0.636 | 15.735 | 5.664 | 103.9 | 37.2 |
| 310 | 0.631 | 15.847 | 5.533 | 106.3 | 37.7 |
| 312 | 0.627 | 15.958 | 5.403 | 108.9 | 38.1 |
| 314 | 0.622 | 16.069 | 5.275 | 111.5 | 38.6 |
| 316 | 0.618 | 16.180 | 5.149 | 114.3 | 39.0 |
| 318 | 0.614 | 16.291 | 5.024 | 117.1 | 39.5 |
| 320 | 0.610 | 16.401 | 4.900 | 120.0 | 40.0 |
| 322 | 0.606 | 16.511 | 4.778 | 123.1 | 40.5 |
| 324 | 0.602 | 16.621 | 4.658 | 126.3 | 41.0 |
| 326 | 0.598 | 16.731 | 4.539 | 129.6 | 41.6 |
| 328 | 0.594 | 16.840 | 4.422 | 133.0 | 42.1 |
| 330 | 0.590 | 16.948 | 4.307 | 136.6 | 42.7 |
| 332 | 0.586 | 17.056 | 4.193 | 140.3 | 43.2 |
| 334 | 0.583 | 17.164 | 4.082 | 144.1 | 43.8 |
| 336 | 0.579 | 17.271 | 3.972 | 148.1 | 44.4 |
| 338 | 0.575 | 17.377 | 3.864 | 152.2 | 45.1 |
| 340 | 0.572 | 17.482 | 3.757 | 156.6 | 45.7 |
| 342 | 0.569 | 17.586 | 3.653 | 161.0 | 46.3 |
| 344 | 0.565 | 17.689 | 3.550 | 165.7 | 47.0 |
| 346 | 0.562 | 17.791 | 3.449 | 170.5 | 47.7 |
| 348 | 0.559 | 17.892 | 3.350 | 175.6 | 48.4 |
| 350 | 0.556 | 17.991 | 3.253 | 180.8 | 49.1 |
| 352 | 0.553 | 18.089 | 3.158 | 186.3 | 49.8 |
| 354 | 0.550 | 18.184 | 3.065 | 191.9 | 50.6 |
| 356 | 0.547 | 18.278 | 2.973 | 197.9 | 51.4 |
| 358 | 0.544 | 18.370 | 2.883 | 204.0 | 52.2 |
| 360 | 0.542 | 18.459 | 2.796 | 210.4 | 53.0 |
| 362 | 0.539 | 18.545 | 2.710 | 217.1 | 53.8 |
| 364 | 0.537 | 18.629 | 2.626 | 224.0 | 54.7 |
| 366 | 0.534 | 18.709 | 2.543 | 231.3 | 55.5 |
| 368 | 0.532 | 18.786 | 2.463 | 238.8 | 56.4 |

| | | | | | |
|---|---|---|---|---|---|
| 370 | 0.530 | 18.859 | 2.385 | 246.7 | 57.4 |
| 372 | 0.528 | 18.929 | 2.308 | 254.9 | 58.3 |
| 374 | 0.527 | 18.993 | 2.233 | 263.5 | 59.3 |
| 376 | 0.525 | 19.053 | 2.160 | 272.4 | 60.3 |
| 378 | 0.523 | 19.108 | 2.088 | 281.7 | 61.3 |
| 380 | 0.522 | 19.157 | 2.019 | 291.4 | 62.3 |
| 382 | 0.521 | 19.201 | 1.951 | 301.6 | 63.4 |
| 384 | 0.520 | 19.238 | 1.884 | 312.2 | 64.5 |
| 386 | 0.519 | 19.268 | 1.820 | 323.2 | 65.6 |
| 388 | 0.518 | 19.291 | 1.757 | 334.8 | 66.8 |
| 390 | 0.518 | 19.306 | 1.696 | 346.8 | 68.0 |
| 392 | 0.518 | 19.312 | 1.636 | 359.5 | 69.2 |
| 394 | 0.518 | 19.311 | 1.579 | 372.7 | 70.5 |
| 396 | 0.518 | 19.299 | 1.522 | 386.4 | 71.8 |
| 398 | 0.519 | 19.278 | 1.467 | 400.9 | 73.1 |
| 400 | 0.520 | 19.247 | 1.414 | 415.9 | 74.5 |

**Table 7-3.** Rates of CO and $CO_2$ production as a function of wavelength calculated using equations 7-8–7-9.

| λ/nm | $10^4 \times dCO/dt$ (ppbv) | $10^4 \times dCO_2/dt$ (ppmv) | | |
|---|---|---|---|---|
| | | inshore | open ocean | costal |
| 200 | 25.008 | 2.551 | 7.898 | 3.444 |
| 202 | 34.854 | 3.496 | 11.249 | 4.858 |
| 204 | 40.328 | 3.977 | 13.302 | 5.689 |
| 206 | 41.792 | 4.052 | 14.087 | 5.966 |
| 208 | 41.107 | 3.918 | 14.161 | 5.939 |
| 210 | 39.556 | 3.707 | 13.926 | 5.784 |
| 212 | 37.730 | 3.476 | 13.574 | 5.584 |
| 214 | 35.862 | 3.248 | 13.186 | 5.371 |
| 216 | 34.039 | 3.031 | 12.790 | 5.160 |
| 218 | 32.290 | 2.827 | 12.400 | 4.954 |
| 220 | 30.623 | 2.636 | 12.017 | 4.755 |
| 222 | 29.037 | 2.457 | 11.645 | 4.563 |
| 224 | 27.530 | 2.290 | 11.284 | 4.378 |
| 226 | 26.099 | 2.135 | 10.932 | 4.201 |
| 228 | 24.741 | 1.989 | 10.590 | 4.030 |
| 230 | 23.451 | 1.854 | 10.259 | 3.866 |
| 232 | 22.226 | 1.728 | 9.936 | 3.709 |
| 234 | 21.064 | 1.610 | 9.624 | 3.557 |
| 236 | 19.960 | 1.500 | 9.320 | 3.412 |
| 238 | 18.913 | 1.397 | 9.025 | 3.272 |
| 240 | 17.919 | 1.301 | 8.738 | 3.137 |
| 242 | 16.976 | 1.212 | 8.460 | 3.008 |
| 244 | 16.081 | 1.129 | 8.190 | 2.884 |
| 246 | 15.232 | 1.051 | 7.928 | 2.764 |
| 248 | 14.426 | 0.979 | 7.673 | 2.650 |
| 250 | 13.662 | 0.911 | 7.426 | 2.540 |
| 252 | 12.937 | 0.848 | 7.187 | 2.434 |
| 254 | 12.249 | 0.790 | 6.954 | 2.332 |
| 256 | 11.597 | 0.735 | 6.728 | 2.235 |
| 258 | 10.978 | 0.684 | 6.509 | 2.141 |
| 260 | 10.391 | 0.637 | 6.296 | 2.051 |
| 262 | 9.835 | 0.592 | 6.090 | 1.965 |
| 264 | 9.308 | 0.551 | 5.890 | 1.882 |
| 266 | 8.807 | 0.513 | 5.696 | 1.802 |
| 268 | 8.333 | 0.477 | 5.508 | 1.726 |
| 270 | 7.884 | 0.444 | 5.325 | 1.652 |
| 272 | 7.458 | 0.413 | 5.148 | 1.582 |
| 274 | 7.054 | 0.384 | 4.976 | 1.514 |
| 276 | 6.672 | 0.357 | 4.810 | 1.450 |
| 278 | 6.310 | 0.332 | 4.649 | 1.387 |
| 280 | 5.966 | 0.308 | 4.492 | 1.328 |
| 282 | 5.641 | 0.287 | 4.340 | 1.271 |

| | | | | |
|---|---|---|---|---|
| 284 | 5.333 | 0.266 | 4.193 | 1.216 |
| 286 | 5.041 | 0.248 | 4.051 | 1.163 |
| 288 | 4.764 | 0.230 | 3.913 | 1.112 |
| 290 | 4.503 | 0.214 | 3.779 | 1.064 |
| 292 | 4.255 | 0.199 | 3.649 | 1.018 |
| 294 | 4.020 | 0.184 | 3.524 | 0.973 |
| 296 | 3.798 | 0.171 | 3.402 | 0.930 |
| 298 | 3.588 | 0.159 | 3.284 | 0.889 |
| 300 | 3.388 | 0.148 | 3.170 | 0.850 |
| 302 | 3.200 | 0.137 | 3.060 | 0.813 |
| 304 | 3.022 | 0.127 | 2.953 | 0.777 |
| 306 | 2.853 | 0.118 | 2.849 | 0.742 |
| 308 | 2.693 | 0.110 | 2.749 | 0.709 |
| 310 | 2.542 | 0.102 | 2.651 | 0.677 |
| 312 | 2.400 | 0.094 | 2.557 | 0.647 |
| 314 | 2.264 | 0.088 | 2.466 | 0.618 |
| 316 | 2.137 | 0.081 | 2.378 | 0.590 |
| 318 | 2.016 | 0.075 | 2.293 | 0.563 |
| 320 | 1.901 | 0.070 | 2.211 | 0.538 |
| 322 | 1.793 | 0.065 | 2.131 | 0.514 |
| 324 | 1.691 | 0.060 | 2.053 | 0.490 |
| 326 | 1.595 | 0.056 | 1.979 | 0.468 |
| 328 | 1.503 | 0.052 | 1.906 | 0.446 |
| 330 | 1.417 | 0.048 | 1.837 | 0.426 |
| 332 | 1.336 | 0.044 | 1.769 | 0.406 |
| 334 | 1.259 | 0.041 | 1.703 | 0.387 |
| 336 | 1.186 | 0.038 | 1.640 | 0.369 |
| 338 | 1.117 | 0.035 | 1.579 | 0.352 |
| 340 | 1.052 | 0.033 | 1.520 | 0.336 |
| 342 | 0.991 | 0.030 | 1.463 | 0.320 |
| 344 | 0.933 | 0.028 | 1.407 | 0.305 |
| 346 | 0.878 | 0.026 | 1.354 | 0.290 |
| 348 | 0.826 | 0.024 | 1.302 | 0.277 |
| 350 | 0.778 | 0.022 | 1.252 | 0.263 |
| 352 | 0.731 | 0.021 | 1.204 | 0.251 |
| 354 | 0.688 | 0.019 | 1.157 | 0.239 |
| 356 | 0.647 | 0.018 | 1.112 | 0.227 |
| 358 | 0.608 | 0.016 | 1.068 | 0.216 |
| 360 | 0.572 | 0.015 | 1.026 | 0.206 |
| 362 | 0.537 | 0.014 | 0.985 | 0.195 |
| 364 | 0.504 | 0.013 | 0.946 | 0.186 |
| 366 | 0.474 | 0.012 | 0.907 | 0.177 |
| 368 | 0.445 | 0.011 | 0.871 | 0.168 |
| 370 | 0.417 | 0.010 | 0.835 | 0.159 |
| 372 | 0.391 | 0.009 | 0.800 | 0.151 |
| 374 | 0.367 | 0.009 | 0.767 | 0.144 |
| 376 | 0.344 | 0.008 | 0.735 | 0.136 |
| 378 | 0.322 | 0.007 | 0.704 | 0.129 |
| 380 | 0.302 | 0.007 | 0.674 | 0.122 |
| 382 | 0.283 | 0.006 | 0.645 | 0.116 |
| 384 | 0.265 | 0.006 | 0.617 | 0.110 |

| | | | | |
|---|---|---|---|---|
| 386 | 0.248 | 0.005 | 0.589 | 0.104 |
| 388 | 0.231 | 0.005 | 0.563 | 0.098 |
| 390 | 0.216 | 0.004 | 0.538 | 0.093 |
| 392 | 0.202 | 0.004 | 0.513 | 0.088 |
| 394 | 0.189 | 0.004 | 0.489 | 0.083 |
| 396 | 0.176 | 0.003 | 0.467 | 0.078 |
| 398 | 0.164 | 0.003 | 0.444 | 0.074 |
| 400 | 0.153 | 0.003 | 0.423 | 0.070 |
| $0.58 \times \Sigma$ | 541.416 | 42.032 | 274.528 | 94.763 |

**References**

1- Thompson, M. G. Energetic muons. In *Cosmic Rays at Ground Level*; Wolfendale, A. W., Ed.; The Institute of Physics: London, 1973; pp. 17.

2- Jelley, J. V. *Cerenkov Radiation*; Pergamon: New York, 1958.

3- Andres, E.; Askebjer, P.; Bai, X.; et al. *Nature* **2001**, *410*, 441.

4- AMANDA Collaboration. *Nucl. Instr. Meth. in Phys. Res. Sec. A* **2006**, *556*, 169.

5- AMANDA Collaboration. *Appl. Optics* **1997**, *36*, 4168.

6- Miocinovic, P.; Price, P. B.; Bay, R. C. *Appl. Opt.* **2001**, *40*, 2515.

7- Desideri, P. G.; Lepri, L.; Udisti, R.; Checchini, L.; Del Bubba, M.; Cini, R.; Stortini, A. M. *Internat. J. Environ. Anal. Chem.* **1998**, *71*, 331.

8- Domine, F.; Shepson, P. B. *Science* **2002**, *297*, 1506.

9- Gayley, R. I.; Ram, M. *J. Geophys. Res.* **1985**, *90*, 12921.

10- Kawamura, K.; Kasukabe, H.; Yasui, O.; Barrie, L. A. *Geophys. Res. Lett.* **1995**, *22*, 1253.

11- Kawamura, K.; Yokoyama, K.; Fujii, Y.; Watanabe, O. *J. Geophys. Res.* **2001**, *106*, 1331.

12- Savarino, J.; Legrand, M. *J. Geophys. Res.* **1998**, *103*, 8267.

13- Grannas, A. M.; Hockaday, W. C.; Hatcher, P. G.; Thompson, L. G.; Mosley-Thompson, E. *J. Geophys. Res.* **2006**, *111*, D04304.

14- Gao, H. Z.; Zepp, R. G. *Env.Sci. & Technol.* **1998**, *32*, 2940.

15- Miller, W. L.; Zepp, R. G. *Geophys. Res. Lett.* **1995**, *22*, 417.

16- Moran, M. A.; Zepp, R. G. *Limnol. and Oceanogr.* **1997**, *42*, 1307.

17- Opsahl, S. P.; Zepp, R. G. *Geophys. Res. Lett.* **2001**, *28*, 2417.

18- Valentine, E. L.; Zepp, R. G. *Environm. Sci. Technol.* **1993**, *27*, 409.

19- Kawamura, K.; Yokoyama, K.; Fujii, Y.; Watanabe, O. *J. Geophys. Res.* **2001**, *106*, 1331.

20- Wang, H.; Kawamura, K.; Yamazaki, K. *J. Atmos. Chem.* **2006**, *53*, 43.

21- Kawamura, K.; Imai, Y.; Barrie, L. A. *Atmos. Environ.* **2005**, *39*, 599.

22- Kawamura, K.; Kasukabe, H.; Barrie, L. A. *Atmos. Environ.* **1996**, *30*, 1709.

23- Guzmán, M. I.; Colussi, A. J.; Hoffmann, M. R. *J. Geophys. Res.* **2006**, Submitted.

24- Petit, J. R.; et al. *Nature* **1999**, *399*, 429.

25- Zuo, Y. G.; Jones, R. D. *Water Research* **1997**, *31*, 850.

26- Osburn, C. L.; Morris, D. P.; Thorn, K. A.; Moeller, R. E. *Biogeochemistry* **2001**, *54*, 251.

27- Grannas, A. M.; Shepson, P. B.; Filley, T. R. *Global Biogeoch. Cycles* **2004**, *18*, GB1006.

28- Mopper, K.; Zhou, X.; Kieber, R. J.; Kieber, D. J.; Sikorski, R. J.; Jones, R. D. *Nature* **1991**, *353*, 60.

29- Schade, G. W.; Hofmann, R. M.; Crutzen, P. J. *Tellus* **1999**, *51 B*, 889.

30- Johannessen, S. C.; Miller, W. L. *Marine Chemistry* **2001**, *76*, 271.

31- Askebjer, P.; Barwick, S. W.; Bergstrom, L.; et al. *Geophys. Res. Lett.* **1997**, *24*, 1355.

32- Anklin, M.; Barnola, J. M.; Schwander, J.; Stauffer, B.; Raynaud, D. *Tellus* **1995**, *47 B*, 461.

33- Colussi, A. J.; Hoffmann, M. R. *Geophys. Res. Lett.* **2003**, *30*, 1195.

34- Haan, D.; Raynaud, D. *Tellus* **1998**, *50 B*, 253.